13th Australasian Fluid Mechanics Conference
Monash University, Melbourne, Australia
13-18 December 1998

PLANAR LASER-INDUCED FLUORESCENCE THERMOMETRY IN A HYPERSONIC BOUNDARY LAYER FLOW

P.C. PALMA,* S.G. MALLINSON, S. O'BYRNE* and P.M. DANEHY***

*Department of Physics and Theoretical Physics, The Faculties, The Australian National University, Canberra ACT, AUSTRALIA

**Faculty of Engineering, University of Technology Sydney, Broadway NSW, Australia

ABSTRACT

Planar laser-induced fluorescence (PLIF) measurements are performed in a hypersonic boundary layer flow over a flat plate at zero incidence. The boundary layer thickness is approximately 1 mm at a distance of 75 mm from the leading edge for this Mach 7.5 nitrogen flow. The temperature variations within the boundary layer are satisfactorily resolved using PLIF. Reduction of the experimental data to produce a temperature profile across the boundary layer shows good agreement with predictions from a high-resolution Navier-Stokes solver.

INTRODUCTION

The boundary layer flow over hypersonic vehicles plays a significant role in determining the performance of engine inlets, lifting surfaces and control flaps. It is therefore critical to have a detailed understanding of relatively simple boundary-layer flows, such as that which develops over a flat plate, to assess possible design input limitations for these systems. One characteristic of hypersonic flows encountered in practical situations is the presence of so-called "real-gas" effects, such as dissociation and vibrational relaxation. These processes can be particularly important in hypersonic boundary layers, where viscous heating can raise the temperature to many times that experienced in the main-stream flow. Despite this fact, there have been few experimental studies of hypervelocity (that is, high-enthalpy and hypersonic) boundary-layer flows where real-gas effects are significant.

Previously, measurements of surface pressure and heat transfer under hypervelocity conditions have been found to agree well with theoretical predictions (East et al, 1980; Mallinson et al., 1997). In contrast, measurements of the density profile have found an apparent surfeit of density in the boundary layer (Baird, et al., 1985; Mallinson et al., 1996), with compressible boundary-layer theory under-predicting the measurements by up to 50%. At first glance, this would appear to be caused by chemical and vibrational nonequilibrium induced by viscous heating. However, rate calculations indicate that these processes cannot be used to explain the observed discrepancy. Further, experiments on low-enthalpy boundary-layer flows have also measured densities greater than those predicted by boundary-layer theory. A possible explanation for this disagreement is that the measurements were performed using a line-of-sight technique: Mach-Zehnder interferometry. Flow spillage from the sides of the model would therefore have caused the effective optical path length to be smaller than for an ideal two-dimensional flow. The density varies inversely with optical path length and so spillage would result in higher density being observed.

One way to obtain data which is free from edge effects is to use a technique that gives a cross-section or slice through the flow, such as planar laser-induced fluorescence (PLIF) (Eckbreth, 1996). For this reason we have performed PLIF thermometry on a hypersonic flow over a flat plate to resolve the discrepancies between experimental boundary-layer profile data and theoretical predictions at hypersonic conditions. The flow is generated using a free-piston shock tunnel (Stalker, 1967). This facility is capable of producing a high-enthalpy, high Mach number free-stream flow in which real-gas effects can be appreciable. For this preliminary study, however, we have chosen to focus on a flow condition which is chemically and vibrationally frozen to separate the fluid dynamics from the molecular physics of the flow.

COMPUTATIONAL METHOD

The flow is computed using a high-resolution Navier-Stokes solver, the full details of which are presented elsewhere (Hillier, 1991; Mallinson et al., 1997). The equations are discretized using a finite-volume approach on a structured grid and are solved using an operator split algorithm, whereby the inviscid and viscous parts of the flow are solved separately. The permits the solver to proceed at the optimum time-step for each part of the flow. The overall solver is second-order accurate in both space and time for smooth regions. For the present computations, the flow is treated as a perfect gas with constant ratio of specific heats, $\gamma = 1.4$.

The mesh is 151x81 in the stream-wise and transverse directions, respectively. Computations with double the number of cells showed only minor differences. The mesh is refined to capture the leading-edge region and wall stretching is applied so that the centre of the first cell lies at $y^+ = y\, U_\tau / \nu < 3$, which is sufficient to capture the near wall behaviour for laminar flows. Here, y is the normal distance from the surface, $U_\tau = (\tau_w / \rho)^{1/2}$ is the friction velocity $\nu = \mu / \rho$ is the kinematic viscosity, $\tau_w = \mu\, (\partial u/\partial y)_w$ is the wall shear stress, ρ is the density, μ is the molecular viscosity and u is the velocity. The subscript 'w' denotes conditions evaluated at the wall.

The computed temperature field for the present flow is shown in Figure 1. The weak leading edge shock causes the temperature to rise by a few degrees. The boundary layer grows rapidly near the leading edge corresponding to the strong interaction region. By about $x = 10$ mm, the

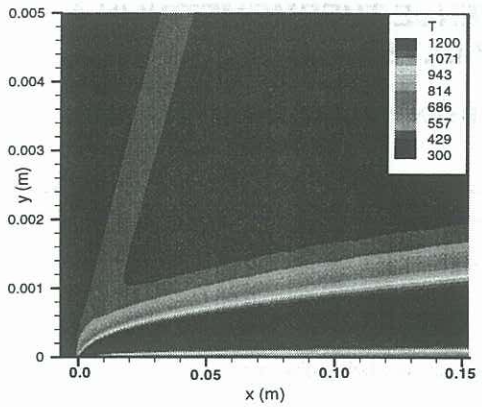

Figure 1. Theoretical temperature map for flat-plate flow. In this figure the vertical length scale is expanded to allow easier viewing.

boundary layer growth is more gradual, corresponding to the weak interaction region, wherein the experiments were conducted. The temperature rises from the edge of the boundary layer until it reaches a maximum close to the wall. Thereafter, the temperature decreases until it reaches the wall temperature, as expected from boundary-layer theory (see, for example, Mallinson et al (1996)).

EXPERIMENTAL METHOD

Flow Conditions and Model

The experiments were performed using the T2 free-piston shock tunnel at the Australian National University. A description of the shock tunnel and its operation is given by Stalker (1967). The T2 nozzle has a 15-degree full-angle conical geometry with a 6.4 mm diameter throat and an exit-to-throat area ratio of 144.

The primary shock speed was 2.4 km s^{-1} which corresponds to a flow total enthalpy of 5.3 MJ kg^{-1}. The nozzle-reservoir pressure was measured to be 27.9 MPa whilst the reservoir temperature was calculated to be 4500 K using the equilibrium shock tube code ESTC (McIntosh, 1968). The nozzle-exit conditions were calculated using the quasi-one dimensional nonequilibrium nozzle-flow code STUBE (Vardavas, 1984). The free-stream conditions were: velocity u_∞ = 2.9 km s^{-1}; static temperature T_∞ = 410 K; density ρ_∞ = 0.04 kg m^{-3}; and Mach number M_∞ = 7.5. The test gas was mostly nitrogen (98.9% N_2 and 1.1% O_2 in the shock tube, resulting in 98.1% N_2, 1.1% NO, 0.4% O_2, and 0.3% O in the test section). The flow at the nozzle exit was both chemically and vibrationally frozen.

The flat plate model is equipped with a sharp leading edge. Its chord and span are 120 mm and 50 mm, respectively. It is oriented such that the laser sheet coincides with the centre-line of the plate. The model was placed at a zero angle of attack, and the leading edge was located 15 mm upstream of the nozzle exit plane, which is equivalent to 240 mm from the nozzle throat.

Planar Laser-Induced Fluorescence

PLIF is a spectroscopic technique that uses a thin sheet of laser light to excite absorption transitions of a particular chemical species in the flow. Some of the absorbed light is emitted as fluorescence and is collected at right angles to the sheet with a two dimensional electronic detector. By collecting this signal for two or more different molecular transitions, the two-dimensional rotational and vibrational temperature fields may be evaluated (Eckbreth, 1996; Palma, 1998).

Here we employ nitric oxide (NO) excitation due to its well-characterized spectroscopy and desirable properties for thermometry. NO occurs naturally in air (in very small concentrations) but can be seeded into flows if necessary. In the current experiment the NO is produced when the shock wave formed after rupture of the primary diaphragm reflects from the end wall of the shock tube at the entrance to the nozzle. In this area, known as the nozzle-reservoir region, the gas temperature and pressure levels are very high. If a small amount of O_2 is present in the N_2 test gas at these conditions, it will dissociate and form NO. Therefore, in the current experiments, about 1% of the test gas is O_2. This eliminates the hazards of handling NO, which is toxic.

The experimental arrangement is shown in Figure 2. The output of an excimer-pumped dye laser was frequency doubled to obtain approximately 5 mJ near 226 nm. This wavelength coincides with the (0,0) $A^2\Sigma^+ \leftarrow X^2\Pi$ vibrational transition of NO. Part of the beam was split off and the wavelength calibrated by performing LIF in a flame. The laser line-width was measured to be 0.18 cm^{-1} by performing LIF in a low-pressure room-temperature cell. The remaining laser energy was formed into a laser sheet using a 40 mm-cylindrical and a 1000 mm-spherical lens. The sheet was measured to be approximately 0.6 mm thick by traversing a knife edge through the sheet while measuring the transmitted beam intensity with a photo-diode.

The collection optics are the main difference between this experiment and previous PLIF experiments (Palma, 1998; Palma et al, 1998). Because the boundary layer thickness is only approximately 1 mm for the current flow conditions, the magnification of the collection optics had to be increased in order to resolve the variation in signal across the boundary layer. The camera used in these experiments is an intensified CCD camera (Princeton Instruments, 576 × 384 pixels) with a 105-mm-focal-length Nikor UV lens. The camera may be gated down to 50 ns to eliminate background interference. In the current experiments this was not

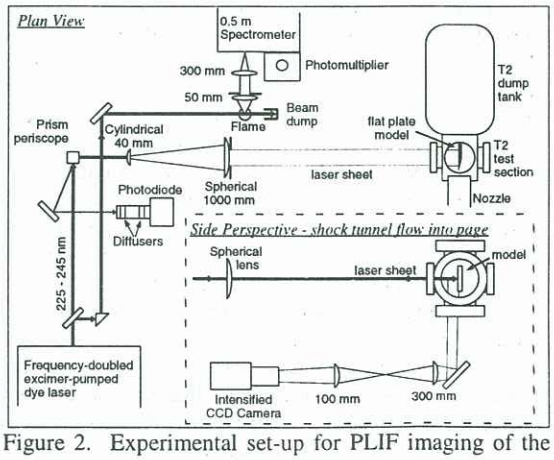

Figure 2. Experimental set-up for PLIF imaging of the boundary layer on a flat plate.

necessary and a 1 μs gate was employed. The maximum resolution that may be obtained without modifications to the camera system is about 10 pixels per mm. To improve this, two extra UV lens were used in conjunction with the camera lens to increase the magnification. A 300 mm focal-length lens was employed to produce a magnified real image of the flow. This image was directed onto the camera by a 100 mm focal-length lens. This lens combination allowed a region of 12 mm × 8 mm to fill the CCD, producing a resolution of approximately 45 pixels per mm. Elastic scatter at the laser wavelength was blocked by using a 3 mm thick UG5 Schott glass filter. The imaged region was located at 75 mm from the leading edge of the flat plate.

Spatial calibration was achieved by introducing a small amount of NO into a N_2 bath in the test section and performing PLIF on the static gas sample. A 5 mm wide section of the laser sheet was blocked, producing a PLIF signal with a known spatial variation (see Figure 3). This was used to determine the magnification of the imaging system.

A measurement of the LIF saturation irradiance was also performed by measuring the PLIF signal as a function of laser-sheet energy. The $R_2(26.5)$ transition was found to have a saturation irradiance of 178 kW cm^{-2}. From this measurement, where the static gas conditions were 296 K and 1.35 kPa, the saturation irradiance for other NO transitions and other conditions was determined. For the laser irradiance values used in the current experiments, the level of saturation was approximately 50%. These high levels of irradiance were necessary because of additional losses introduced by the magnifying lenses.

The experimental procedure was as follows. Prior to each tunnel run the laser was tuned to the chosen NO transition by performing LIF in the flame. When the tunnel was fired, a pressure transducer detected the arrival of the primary shock wave and triggered the laser and camera after a suitable delay. Five images were obtained, in separate tunnel runs, for each of the transitions employed. These measurements were averaged to produce the final result. Because the laser energy was held constant and each transition had the same degree of saturation, the effect of saturation is removed when the temperature is determined. The final result is obtained by averaging the signal in the stream-wise direction. Because flow gradients over the 8 mm region are small, this results in only minor measurement errors.

RESULTS and DISCUSSION

The PLIF signals obtained from two different NO transitions are shown in Figure 4 as a function of the normal distance from the flat plate. The cross sections are taken at a distance $x = 75$ mm from the leading edge of the flat plate. The magnitude of the signal for the $P_1(35.5)$ transition has been scaled to fit onto the figure. Also shown are the calculated PLIF signals based on the computational predictions of the flow. It is difficult to convert the measured signal to physical units. However, the profiles have been scaled appropriately so that the measured free-stream signal levels agree with the calculated values. This is reasonable because for the determination of the temperature profile, it is the ratio of

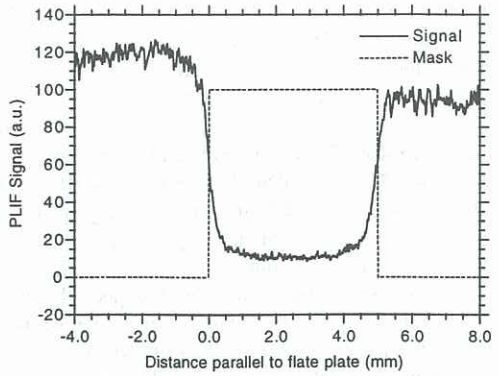

Figure 3. A 5 mm-wide mask is inserted in the beam to provide a spatial calibration of the imaging system from which the resolution of the imaging system is estimated.

the signals from the two transitions that is important (Palma, 1998).

It can be seen that the measured signals fall below the calculated values in the boundary layer, whilst at the edge of the boundary layer, the $P_1(35.5)$ signal level is greater than that predicted. Also, the boundary layer appears broadened or smeared out in comparison with the calculated values. These two observations imply that the spatial resolution of the imaging is insufficient to completely resolve the features of the boundary layer. We believe that this reduced resolution is caused by chromatic aberrations from the extra two lenses used to increase the magnification of the imaging system. The measured PLIF signal for $y < 0$ mm (inside the wall) is due to reflection of fluorescence from the plate. This also contributes to the signal not reaching the wall temperature, 295 K, at $y = 0$ mm.

While performing PLIF tests on stagnant NO in the test section, we observed that the laser scatter from the surface of the model could be sharply focused to form a 100 μm (2 pixel) feature. However, as shown in Figure 3, we were unable to achieve a tight focus with the PLIF signal; instead, the sharp edge of the blocked laser sheet was smeared across approximately 0.5 mm. We believe this is because the fluorescence signal is broadband, covering approximately 40 nm, as opposed to the laser scatter which is virtually monochromatic. Hence we conclude that the current imaging system cannot spatially resolve all of the features in the boundary layer.

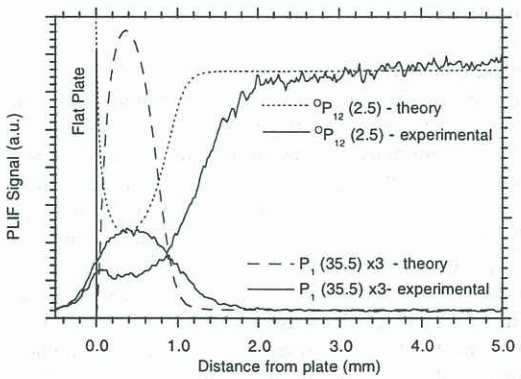

Figure 4. PLIF signal as a function of normal distance from the surface of the flat plate. The cross section through the boundary layer is taken at $x = 75$ mm.

The two transitions used here, the $^{O}P_{12}(2.5)$ and the $P_1(35.5)$, allow excellent temperature sensitivity due to the large difference in the energies ΔE of their absorbing rotational levels. The rotational temperature is calculated and shown in Figure 5. The measured free-stream temperature of 400±20 K is in excellent agreement with the value of 410 K calculated using STUBE. The measured peak temperature in the boundary layer is 1000±100 K, which is in fair agreement with the theoretically predicted maximum of 1180 K. Due to the reduced spatial resolution, one would expect the true peak temperature in the boundary layer to be slightly larger than the measured value, as is observed. Overall, the agreement between experiment and computation is good, with both the general trend and the levels matching closely.

Considering the previous measurements (Baird et al, 1985; Mallinson et al, 1996), the minimum density in the boundary layer (which occurs at the same location as the maximum temperature) was double that predicted by boundary layer theory. The pressure across the boundary layer will be very nearly constant, and so this corresponds to predicting a maximum temperature twice that observed in experiment. The present observations therefore imply that the line-of-sight measurement technique employed in the earlier studies, namely Mach-Zehnder interferometry, was indeed affected by flow spillage at the edges of the plate. The PLIF technique, which captures a two-dimensional slice through the flow, does not suffer from this problem.

The main sources of uncertainty in this thermometry method are due to laser-mode fluctuations. The pulse-to-pulse variation in the PLIF signal due to mode fluctuations is about 25% at the conditions encountered in the free-stream. By averaging over several images for each transition, and using the favourable value of $\Delta E/kT$ (7.3 in the free-stream and 2.9 in the boundary layer), the uncertainties are significantly reduced.

The high level of saturation requires certain assumptions to be made about the PLIF signals. If the level of saturation can be kept the same for all images, then these effects cancel out in the temperature calculation. In the current experiments the laser energies varied by 10% between images. At saturation levels of 50% this translates into approximately a 3% error in the signal, and is therefore negligible compared with laser-mode fluctuations.

CONCLUSIONS

Temperature measurements in a chemically- and vibrationally-frozen hypersonic laminar boundary layer have been presented. The measurements show good agreement with the predictions from a high resolution Navier-Stokes solver. The success of this preliminary study indicates that more extensive measurements are feasible. In particular, the study of real-gas effects on boundary layers can now be undertaken with reasonable confidence in the PLIF measurement system. However, improvements to the imaging system (to reduce chromatic aberrations) are necessary to resolve flow features less than 0.5 mm in size. This may not be a problem in larger facilities, such as the T3 shock tunnel, where the model length can be greatly increased resulting in a much larger value of boundary layer thickness. In conclusion, this study would seem to indicate that the discrepancies previously observed between measured and calculated density profiles (Baird et al, 1985; Mallinson et al, 1996) are most likely due to flow-spillage affecting the line-of-sight measurement technique.

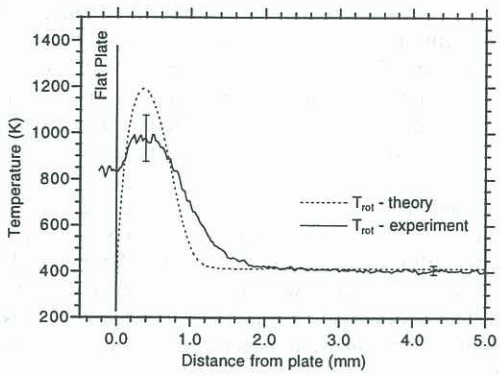

Figure 5. Temperature as a function of normal distance from the flat plate. The cross section through the boundary layer is taken at $x = 75$ mm.

REFERENCES

BAIRD, J.P., LYONS, P.R.A and GAI, S.L., "Density and velocity profiles in non-equilibrium laminar boundary layers in air," *AIAA paper* 85-0976, 1985.

EAST, R.A., STALKER, R.J. and BAIRD, J.P., "Measurements of heat transfer to a flat plate in a dissociated high-enthalpy laminar air flow," *J. Fluid Mech.*, **97**, 673-699, 1980.

ECKBRETH, A.C., *Laser Diagnostics for Combustion Temperature and Species*, Gordon and Breach, UK 1996.

HILLIER, R., "Computation of shock wave diffraction at a ninety degrees convex edge," *Shock Waves*, **1**, 89-98, 1991.

MALLINSON, S.G., GAI, S.L. and MUDFORD, N.R., "The boundary layer on a flat plate in hypervelocity flow," *Aeronautical J.*, **100**, 135-141, 1996.

MALLINSON, S.G., GAI, S.L. and MUDFORD, N.R., "The interaction of a shock wave with a laminar boundary layer at a compression corner in high enthalpy flows including real gas effects," *J. Fluid Mech.*, **342**, 1-35, 1997.

MALLINSON, S.G., HILLIER, R., ZANCHETTA, M., SOLTANI, S. and KIRK, D., "An experimental and numerical study of hypersonic turbulent boundary layers." *AIAA paper* 97-2290. 1997.

PALMA, P.C., DANEHY, P.M., and HOUWING, A.F.P., "Non-intrusive thermometry in shock layers using multi-line fluorescence imaging," *Proc. 21st Int. Symp. on Shock Waves*, 447-452, 1998.

PALMA, P.C., PhD Thesis, Australian National University, 1998.

STALKER, R.J., "A study of the free-piston shock tunnel," *AIAA J.*, **5(12)**, 2160-2165, 1967.

McINTOSH, M., "Computer program for the numerical calculation of equilibrium and perfect gas conditions in shock tunnels," *Australian Defence Scientific Service WRE Tech Note* CPD 169, 1969.

VARDAVAS I., "Modelling reactive gas flows within shock tunnels," *Aust. J. Phys.*, **37**, 157-177, 1984.